

ACTIVE TRANSFER BAGGING—A NEW APPROACH FOR ACCELERATED ACTIVE LEARNING ACQUISITION OF DATA BY COMBINED TRANSFER LEARNING AND BAGGING BASED MODELS

Vivienne Pelletier^{1,*}, Daniel J. Rivera^{2,*}, Obinna Nwokonkwo², Steven A. Wilson², Christopher L. Muhich ^{1,2†}

¹ Materials Science & Engineering, School for the Engineering of Matter, Transport, & Energy, Arizona State University, 551 E. Tyler Mall, Tempe Arizona, 85287, USA

² Chemical Engineering, School for the Engineering of Matter, Transport, & Energy, Arizona State University, 551 E. Tyler Mall, Tempe Arizona, 85287, USA

ABSTRACT

Modern machine learning has achieved remarkable success on many problems, but this success often depends on the existence of large, labeled datasets. While active learning can dramatically reduce labeling cost when annotations are expensive, early performance is frequently dominated by the initial seed set, typically chosen at random. In many applications, however, related or approximate datasets are readily available and can be leveraged to construct a better seed set. We introduce a new method for selecting the seed data set for active learning, Active-Transfer Bagging (ATBagging). ATBagging estimates the informativeness of candidate data point from a Bayesian interpretation of bagged ensemble models by comparing in-bag and out-of-bag predictive distributions from the labeled dataset, yielding an information-gain proxy. To avoid redundant selections, we impose feature-space diversity by sampling a determinantal point process (DPP) whose kernel uses Random Fourier Features and a quality-diversity factorization that incorporates the informativeness scores. This same blended method is used for selection of new data points to collect during the active learning phase. We evaluate ATBagging on four real-world datasets covering both target-transfer and feature-shift scenarios (QM9, ERA5, Forbes 2000, and Beijing PM_{2.5}). Across seed sizes $n_{\text{seed}} = 10\text{--}100$, ATBagging improves or ties early active learning and increases area under the learning-curve relative to alternative seed subset selection methodologies in almost all cases, with strongest benefits in low-data regimes. Thus, ATBagging provides a low-cost, high reward means to initiating active learning-based data collection.

Keywords Active Learning · Transfer Learning · Design of Experiments · Bayesian · Coresets

1 INTRODUCTION

The reliance of modern machine learning methodologies on large, fully labeled datasets, i.e. datasets with a target y_i associated with each element of the domain x_i , remains a fundamental bottleneck in their application to new problems. The expense of dataset construction is primarily incurred in the labelling process, leading to an abundance of unlabeled datasets [1, 2] particularly when labelling requires consultation with experts, e.g. doctors classifying medical imagery, or when the prediction target is experimentally or computationally demanding to acquire.[3, 4, 5, 6] This expensive data collection process must be repeated if a different target is desired, even when the underlying labels are consistent and the problems are related, i.e. different levels of numerical rigor in a simulation, or a new experimental measurement of the same underlying system. Ameliorating these obstacles requires a rigorous approach towards dataset efficiency, ensuring that labelling and learning expenses are incurred on the fewest representative elements possible.

A common approach to address the expense of data collection is active learning. Active learning is an iterative process where unlabeled data points are selected for acquisition following some criterion, e.g. model uncertainty, model disagreement, or expected change, thereby prioritizing data collection efforts towards the most informative points[7]. However, the quality and effectiveness of this approach is limited by the model's ability to approximate the acquisition criterion from the currently available data set. Thus, the rate of model improvement in the early stages of active learning is dominated by the information content in the model initiation, or seed, data.[8] The seed data is typically chosen via uniform random sampling of the unlabeled pool.[9, 10] Although random sampling is straightforward and not biased by human intuition, it carries no guarantees about the informativeness or representativeness of the resulting seed data set.

We posit that this early inefficiency may be mitigated by recognizing that there often already exist labels of a different prediction target of the data set which are correlated with the target of interest, or at least that there are correlated targets that are easily acquired.[11, 12] In such cases the information provided by these proxy labels should be able to guide the creation of

*These authors contributed equally

†Corresponding author: cmuhich@asu.edu

the model data set seed by finding a transferable, informative subset of the proxy dataset. However, this information is rarely, if at all, used.[13] Therefore, our objective is to leverage the information inherent in proxy datasets to select a seed subset for labelling such that a model trained on the subset gains a broad understanding of the target’s response over the feature space and has well-tuned uncertainty estimates and thus decreases the data sampling during active learning.

A related concept, a coresnet, comes from the field of computational geometry, and is defined as a weighted subset such that the loss of any model evaluated on the coresnet approximates the loss of the full dataset.[14] Coresets are designed to reproduce a specific loss function generally, for all possible models or model parameters; our goal, conversely, is to determine an optimal subset for transferring to a new loss function, such that the predictive performance of a model with optimal parameters trained on the subset is close to that of the same model trained on a full dataset. The coresnet approach is most useful in settings where a large, fully labelled dataset exists but training a model on it is prohibitively expensive. Thus, it is not concerned with the transferability of such a subset to different targets and has not been applied to such tasks.

There remains a major knowledge gap as to how to transfer information from a known dataset to a new, related learning task via the creation of an optimal subset to seed active learning with the new dataset. We call this concept an active transfer learning task and propose that an effective subset for this purpose should maximize two properties: informativeness, i.e. the set of points whose inclusion most affects the model’s predictive distribution, and heterogeneity, i.e. the points which collectively span the feature space.

The first of these has previously been addressed by coresnet generation methodologies and is quantifiable via properties such as influence functions,[15] which estimates the effect of reweighting a training point on model loss or parameters, and sensitivity scores,[16] which quantify how much a training point could contribute to the overall loss across potential model parameter sets. Subset heterogeneity is rarely addressed in the context of dataset pruning, but is often considered in the context of (batch) active learning, where many approaches aim to diversify the selected batch by maximizing the determinant of a covariance matrix,[17] or impose a sampling strategy which iteratively chooses the points with the most distinct uncertainty representation, such as Largest Cluster Maximum Distance.[18] However, these diversifying approaches focus on the model’s predictive uncertainty space rather than the data’s feature space, which we hypothesize will be of greater importance for a transfer task.

While these properties have been addressed separately in different contexts, we combine them into one method that ensures both informative and heterogenous seed subsets for initializing active learning procedures from a transferred data set. Specifically, this work introduces the Active Transfer Bagging (ATBagging) method which combines informativeness scores derived from a Bayesian interpretation of bagged ensemble models with the heterogeneity enforced by determinantal point processes to determine the optimal active learning seed data. In experiments with real world datasets, the ATBagging method is a facile and inexpensive preprocessing step that seeds any active learning method, improves early model uncertainty estimates and accelerates the rate of information acquisition during active learning.

2 METHODS

The proposed ATBagging method contains two major components: 1) the quantification of informativeness and 2) the imposition of subset heterogeneity. In this section we first describe the target class of problems which ATBagging addresses, then we will discuss the mathematics of the two components, and finally we will discuss the real-world datasets and the associated experiments used in benchmarking ATBagging.

2.1 Problem Statement

We consider the transfer learning scenario in which one has access to a source dataset, \mathcal{D} , that consists of labeled data points $\mathcal{D} = (x_i, y_i)_i^N$, where $x_i \in X$ represents a feature vector drawn from sampling distribution $x \sim p(X)$ and $y_i \in Y$ is the corresponding label from the target space Y . Additionally, there is a desired target dataset, \mathcal{D}' , which consists of not-yet-acquired new labels $y'_i \in Y'$ that are correlated with the original labels Y but are expensive or difficult to acquire. The x'_i of \mathcal{D}' may be the same as the x_i of \mathcal{D} , or they may be drawn from a different sampling distribution, $x'_i \sim p'(X)$. Our goal is to construct a small representative subset $\mathcal{S} \subset \mathcal{D}$, such that when training a model to learn the map $f' : X' \rightarrow Y'$ using only \mathcal{S} , its predictive performance approximates the performance of the same model trained on the full dataset \mathcal{D}' .

2.2 Informativeness Scores

We define data point informativeness as the information gain of the predictive distribution $p(Y_*|X_*)$ due to observing the datum (x, y) ,

$$IG_{Y,X}(Y, x) = KL(p(Y_*|X_*, x, y) \parallel p(Y_*|X_*))$$

given by the Kullback-Leibler (KL) divergence[19] between the posterior predictive distribution $p(Y_*|X_*, x, y)$ and the prior predictive distribution $p(Y_*|X_*)$. This definition is oriented towards the predictive information and is a similar definition to the EPIG active learning method.[20] $IG_{Y,X}$ quantifies how much the distribution of the model’s predictions, $p(Y_*|X_*)$, over a set of test inputs, X_* , changes upon incorporation of new observation pairs (x, y) into the model training set. Therefore, X_* should be chosen to be representative of the X set features on which the model will ultimately be applied. Simply using the X set features of the transfer problem, or a subset thereof if it is very large, is a practical approach and we adopt it in this work. However, the creation of full probabilistic models of these distributions for the inclusion and exclusion of every data point would be prohibitively expensive. Instead, a powerful approximation can be found in the Bayesian interpretation of bagged ensemble models.

A bagged ensemble model is a model $\mathcal{M} = \{m_i\}_i^M$, comprised of M submodels of weak learners, m_i , trained on bootstrapped samples of the training dataset.[21] The utility of bagged ensemble models for our purpose comes from interpreting them through an approximate Bayesian lens, where the parameters learned by each submodel m_i are interpreted as Monte Carlo draws from the distribution of model parameters, $p(\theta)$, and therefore their predictions $\tilde{y}_* = m_i(x_*)$ are interpreted as draws from the posterior predictive distribution $\tilde{y}_* \sim p(y_*|x_*, \theta)p(\theta)$. When M is chosen to be sufficiently large (see Appendix A), there exists with very high probability a partitioning of the

submodels into two non-empty subsets whose bootstrapped samples either do or do not contain the training point (x_i, y_i) , called in-bag and out-of-bag models, respectively, and denoted by $\mathcal{M}_{\text{ib}} \subset \mathcal{M}$ and $\mathcal{M}_{\text{oob}} \subset \mathcal{M}$. Both \mathcal{M}_{ib} and \mathcal{M}_{oob} are themselves bagged ensemble models for the datasets \mathcal{D} and $\mathcal{D} \setminus \{(x_i, y_i)\}$ respectively, and therefore their predictions can be interpreted as draws from the posterior predictive distri-

butions $p(Y_*|X_*, x, y)$ and $p(Y_*|X_*)$, the exact distributions required for the definition of information gain.

The approximate samples from these distributions which this interpretation affords allows us to extend this framework and calculate an approximation to the information gain formula. The resulting formula is:

$$\text{KL}(p(Y_*|X_*, x, y) \| p(Y_*|X_*)) = \frac{1}{2} \left[\text{tr}(\Sigma_{\text{oob}}^{-1} \Sigma_{\text{ib}}) + (\mu_{\text{oob}} - \mu_{\text{ib}})^\top \Sigma_{\text{oob}}^{-1} (\mu_{\text{oob}} - \mu_{\text{ib}}) - n - \ln \frac{\det \Sigma_{\text{oob}}}{\det \Sigma_{\text{ib}}} \right]$$

Full mathematical details of the derivation are provided in Appendix B.

2.3 Heterogeneity

For the purposes of an active learning seed subset, we propose that diversity in feature space is important, especially early in the process. However, this cannot come at the expense of informativeness. We therefore use Determinantal Point Processes (DPPs) [22] to balance informativeness and heterogeneity. DPPs provide a method for randomly selecting from a set of points such that more heterogenous subsets are given a higher probability of being sampled, with heterogeneity determined via an imposed similarity measure. DPPs are chosen for this application because the sampling distribution of a DPP is highly customizable; it is possible to emphasize and deemphasize the marginal probability of inclusion of each point individually, and to reduce the heterogeneity bias via weakening the similarity measure. By altering the weight given to these two properties, it is possible to tune the methodology with prior knowledge of the specific application. Even with large datasets, generating samples of a desired size from a DPP can be efficient, thus allowing the entire methodology to be performed in a matter of minutes for datasets of 10-100k labels.

The DPP can be constructed from a matrix L_{ij} whose entries encode the correlations between all (i, j) point pairs in the superset, which is called the L -ensemble. The probability that a subset \mathcal{S} will be sampled from an L -ensemble is given by

$$p(\mathcal{S}) = \frac{\det L_{\mathcal{S}}}{L_{\mathcal{S}} + I}$$

where $L_{\mathcal{S}}$ is the matrix created by selecting only the \mathcal{S} set of rows and columns of L , and I is the identity matrix. This formulation emphasizes sampling of dissimilar points, as the sampling is proportional to the determinant of the correlation matrix. The L -ensemble formulation of a DPP allows the incorporation of the previously determined informativeness scores via the quality-diversity factorization of L proposed by Kulesza [22], while still explicitly considering heterogeneity. This method is chosen over other means of enforcing heterogeneity, i.e. performing biased sampling of groups of spatially clustered data, as it allows a principled way of tuning the importance of informativeness and diversity via alteration of the L matrix construction.

The construction of the DPP and sampling from it require careful consideration. While any correlation structure may be used to construct the L matrix, in our application L is constructed via the Random Fourier Features (RFF) approximation to the

squared exponential kernel,[23] where $k(x, y) = \exp(-\frac{|x-y|^2}{\ell})$ is approximated by $\phi(X)^\top \phi(y)$, with

$$\phi(x) = \sqrt{2/R} [\cos(\omega_r^\top x + b_r)]_{r=1}^R$$

and $\omega_r \sim \mathcal{N}(0, \frac{1}{\ell} I)$ and $b_r \sim \text{Uniform}[0, 2\pi]$ for a predetermined number of features R . This approach was utilized for three reasons: first, it is found to be quicker than calculating the kernel explicitly as it allows the use of fast dot product code. Second, it allows easy application of the quality-diversity factorization of $L_{ij} = q_i \phi_i^\top \phi_j q_j$ by scaling each point's $\phi(x_i)$ by their informativeness score. Third, and most importantly, this affords us the ability to utilize a fast DPP sampling algorithm which we propose in Appendix C.

2.4 ATBagging Algorithm

The combination of information score and heterogeneity is implemented via Algorithm 1, and is shown schematically in Figure 1.

Algorithm 1: Transferable Subset Creation

Data: A dataset $\mathcal{D} = \{(x_i, y_i)\}_i^N$, a bagged ensemble with submodels $\mathcal{M} = \{m_i\}_i^M$, a test set X_* , a desired subset size k

Result: A transferable subset \mathcal{S}

foreach $x_i \in \mathcal{D}$ **do**

$$\mathcal{M}_{\text{ib}} \leftarrow \{m \in \mathcal{M} | x_i \in \tilde{X}_m\}$$

$$\mathcal{M}_{\text{oob}} \leftarrow \{m \in \mathcal{M} | x_i \notin \tilde{X}_m\}$$

Compute $\mu_{\text{ib}}, \mu_{\text{oob}}, \Sigma_{\text{ib}}, \Sigma_{\text{oob}}$ using $\mathcal{M}_{\text{ib}}, \mathcal{M}_{\text{oob}}$ evaluated on the test set X_* (see Appendix B)

$\text{IG}_i \leftarrow \text{KL divergence between in-bag and out-of-bag distributions}$

$$\phi_i \leftarrow \text{RandomFourierFeature}(x_i)$$

end

Initialize matrix L

$$L_{ij} \leftarrow \text{IG}_i \phi_i^\top \phi_j \text{IG}_j$$

$$\mathcal{S} \leftarrow \text{DPPSampler}(L)$$

2.5 Data Sources

We demonstrate the capability of the ATBagging approach to improve machine learning data collection by evaluating its performance on four real-world datasets chosen to address different types of potential applications: 1) the ERA5-Land Hourly

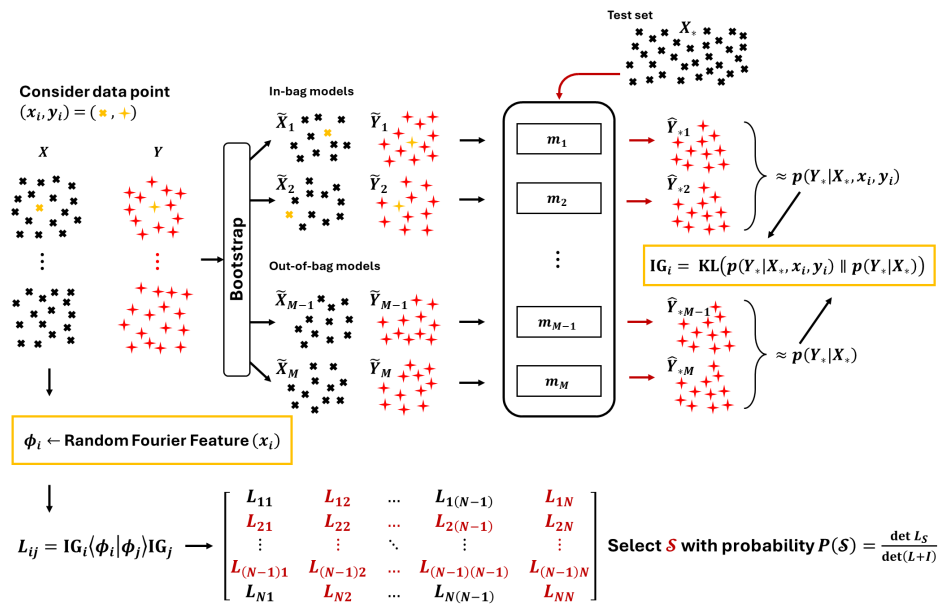


Figure 1: Information flow of the knowledge gain and heterogeneity operators

Weather dataset, [24] 2) the Multi-XC QM9 molecular energy dataset, [25] 3) the Forbes 2000 market evaluation dataset,[26] and 4) the Beijing PM_{2.5} dataset.[27] These data sets were chosen to represent a wide range of possible applications, with varying degrees of X and Y transferability. Additionally, the use of collected rather than synthetic data more accurately represents use cases where sampling error or bias may exist. We partition these datasets into two types according to the transfer problem they address: target-transfer problems and feature-shift problems. Target-transfer problems address situations where the feature set is constant across the transfer (same X 's different Y 's), while feature-shift problems address cases where both the X and Y sets may be different between explored and unexplored domains, with an assumed correlation between them.

The two datasets used to evaluate target-transfer problems are the ERA5-Land Hourly and Multi-XC QM9 datasets. These problems are representative of cases where additional (likely at additional cost) characterization of points is possible, but it is desirable to minimize the cost of additional analysis.

The ERA5-Land Hourly dataset[24] ($N \approx 300,000$) contains six features of surface meteorological measurements. We select the two values related to precipitation as the prediction targets to evaluate the performance of transfer problems. This is an exemplar case of problems where a large dataset has already been collected for one target, total precipitation, but researchers now wish to model a new property of the system, surface runoff. Specifically, we frame this problem as identifying a fixed, small number of locations where meteorologists should measure the new property to gain the most performant and robust model for future predictions.

The Multi-XC QM9 molecular energy database[25] compiles chemical descriptors of $\sim 134,000$ molecules and their energies as calculated by an array of different accuracy quantum chemical methods. This dataset is selected to evaluate target-quality transferability problems, where the true target value is expensive to acquire, but less expensive, poorer, approximations of the target exist. We select the two targets in this test case to be

different in the quality of quantum mechanical approximation used. The transfer target is chosen to be calculations that are roughly 100 times more computationally expensive to acquire, M06-2X functional with a triple-zeta polarized basis, than the low-level method, LDA(VWN) functional with a single-zeta basis. We frame the problem as identifying which molecules the researchers should select for explicit calculation with the expensive method to best predict high quality molecular energies from molecular descriptors.

The two datasets chosen to evaluate domain-shift transfer performance were the Beijing PM_{2.5} dataset and the Forbes dataset. Both these datasets represent problems where the input set is expanded with new unlabeled data of the same type (containing the same features) from a different sampling distribution, i.e. the same features are measured for new data which is collected from a context that is expected to be meaningfully different from that of the original data. For these problems, the subset chosen by our method is determined via identifying the unlabeled points which are closest to the selected points from the original dataset. This is done via either Mahalanobis distance for fully numerical data or k -prototypes distance for mixed numerical-categorical data.[28, 29]

The Beijing PM_{2.5} dataset[27] ($N \approx 40,000$) dataset contains a variety of meteorological measurements which are used to predict the PM_{2.5} concentration (fine particulates which are less than 2.5 micron in diameter) in Beijing from 2010 to 2014. With this dataset, neither the type of features nor the target property change, but the distributions from which the input set is drawn does. This domain split is achieved by dividing the dataset before and after 2012, which is intended to capture the evolution of Chinese pollution regulations. The transfer learning problem is framed as where in Beijing and when during the year it is best to collect meteorological data to maximize the predictive capability for city-wide particulate matter based on information available from previous years.

The Forbes market evaluation dataset[26] provides the sales, profits, assets, industry, location, and market value for just over

Table 1: Summary of Data Sets Used

Data Set	Type	X	Y	Description of Task
QM9	Target transfer	Same	Highly correlated	Selecting transfer subset from dataset with computationally cheap approximation of target to high accuracy calculation
ERA5	Target transfer	Same	Somewhat correlated	Selecting transfer subset from pre-existing dataset when a new target is desired for the same input set
Forbes	Feature shift	Different distributions	Same type	Selecting initial subset to label from newly acquired unlabeled input set which is drawn from a different sampling distribution than the original dataset, but the target remains the same property
PM _{2.5}	Feature shift	Different distributions	Different type	Selecting initial subset to label from newly acquired unlabeled input set which is drawn from a different sampling distribution than the original dataset, and the target is a different property

1500 companies worldwide. The domain split for this problem is constructed by dividing the companies into two classes, Eastern (Asian) and Western (American and European) using Western companies as the available domain and the other as the transfer domain. As these are disjoint divisions (no company is considered both Eastern and Western), the transfer subset is constructed by identifying the closest target companies to the source companies selected by the down-selection method. Thus, the resulting problem is framed as where to best collect information from Asian companies to maximize the predictive performance of their market value, based on information available about Western companies.

2.6 Alternative Methods

To evaluate the effectiveness of our methodology we assess it against three alternative seed data set selection methods. The first is naïve uniform random sampling, which aims to mimic the sampling distribution in feature space. This method takes no information from the existing data. The second is PCA grid sampling, in which the data is transformed via principal component analysis to remove linear correlations and grouped into voxels on a regularly spaced grid, from which points are sampled randomly within each voxel. This ensures feature-space diversity in the resulting subset. This again does not translate target information from the existing data. Finally, we compare performance against a loss-driven coresset methodology, in which data points are selected via importance sampling with probabilities driven by their influence on the model’s loss function, a common approach among simple coresset methodologies.[30] This prioritizes high-impact points to maximize informativeness but does not consider heterogeneity. These baselines span the range of strategies including the naïve approach, an approach addressing only heterogeneity, and an approach addressing only informativeness.

2.7 Performance Evaluation & Metrics

The performance of these methods was evaluated in two related tasks, the downselection of representative subsets of the source dataset and the performance of these subsets for transfer-active learning. We report accuracy, defined as a trial’s r^2 divided

by the maximum r^2 achieved on any trial for that dataset. To summarize the performance of the method across subset sizes we introduce an accuracy vs. subset size curve, normalized such that perfect integrated accuracy is 1. We report the performance as the normalized area under the learning curve (NAULC). Additionally, the proportion of trials in which ATBagging outperformed its competitors is reported, with credible intervals provided via a beta-binomial model of the pairwise comparison data with a Jeffreys prior.[31]

3 RESULTS & DISCUSSION

The goal of ATBagging is use information from available or low collection cost data to seed and drive an active learner. This proceeds through three steps: 1) examination of known points and calculation of their information gain, 2) determination of active learning seed set from the information gain and heterogeneity and 3) active learning of the desired target data. This workflow is shown schematically in Figure 2. We test the performance of each of these processes with the data sets described in Section 2.5. The results of our tests are presented in three subsections. First, we discuss the details of how the methodology was applied, describing the model architecture, active learning algorithm, and justifying the choice of model hyperparameters. Then, we evaluate the quality of the subsets chosen by our method against those of the alternative methods, by first investigating their performance as downselected distillations of the source datasets, followed by their quality as seed subsets for transfer-active learning.

3.1 Experimental Setup

We have chosen to evaluate ATBagging with a bagged ensemble model of 100 decision trees (a random forest regressor, RFR)[32] paired with query-by-committee active learning,[33] with all evaluations being replicated 15 times. The methodology is agnostic to the characteristics of the base model in the bagged ensemble, but decision trees were chosen due to their flexibility and simplicity. Particularly, they can model mixed categorical and continuous features with ease while having low computational demand. Additionally, prior work has demonstrated that, in the active learning context, a bagged ensemble (a random

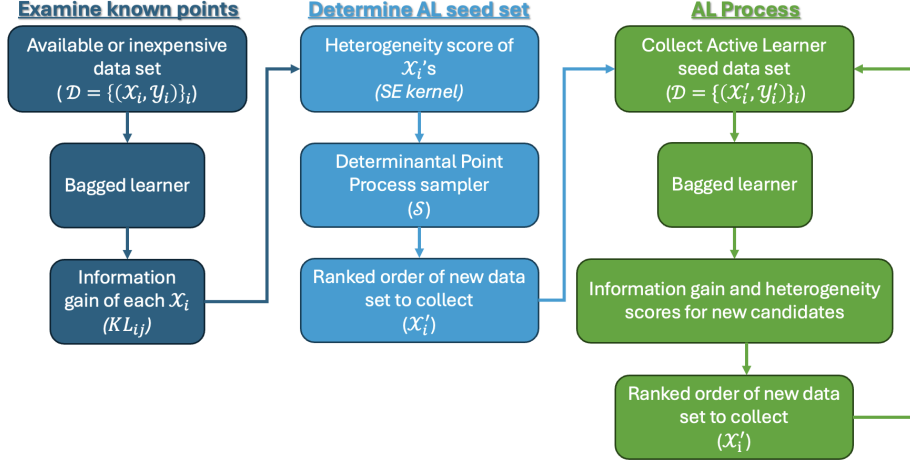


Figure 2: Overview of the three key steps in ATBagging learning approach.

forest) of 100 decision trees performed better than an ensemble of 10 random forests of 10 trees each.[34]

We choose query-by-committee[33] as our active learning methodology as it is a simple, popular approach which is applicable to both regression and classification tasks. Differences in the capabilities of seed set creation methods will be most pronounced at small subset sizes, and problems which require these small subset sizes, ones where label acquisition is extremely expensive, are the applications where this methodology would see the most utility. Therefore, active learning tests are seeded with a small subset size of $n_{\text{seed}} = 10$.

3.2 Model Justification & Performance Characterization

To demonstrate the feasibility of the RFR for the test datasets, we train a model on each dataset and dataset split to be used to evaluate the ATBagging method (e.g. all source and transfer datasets). We employ the python package Scikit-learn[35] to train the RFR model. The entire available dataset is split into an 80/20% train and test set for RFR optimization. Figure 3 shows the parity plot for each RFR model and each dataset considered. We highlight the generally excellent performance of the RFR models on the QM9, PM_{2.5} and Forbes datasets. The RFR model performs worse on the ERA5 weather dataset, but the 0.3 and 0.5 r^2 values are considered strong enough indication that the model is indeed learning, therefore the dataset was included as an example of the methodology's performance on a difficult learning task.

3.3 Downselection

The ability of the different data selection methods to create representative subsets of each source dataset was evaluated. Across datasets, the heterogeneity-aware methods (ATBagging, PCA) retained more source accuracy than informativeness-only (loss coresset). ATBagging was the best or tied for the best performing method in three of the four datasets across all subset sizes tested and was always the best performing method at the smallest subset sizes ($N_{\text{tr}} = 10, 60$).

3.3.1 Downselection Performance: ERA5

The ERA5 dataset was the most difficult of the datasets for the model to learn, and therefore the results on this dataset are characterized via high variance across trials, as seen in the 90% density intervals shown in Figure 4.b. Despite this, ATBagging achieves higher or the same retention of the full dataset training accuracy than the alternatives across all subset sizes tested. The methods that account for the heterogeneity of the selected subset (ATBagging, PCA, and random sampling) outperform the loss coresset method, which prioritizes the informativeness of the selected data points only. These heterogeneity-driven sampling methods retain between 15–50%, 15–46%, and 13–41%, of the full training accuracy on average for ATBagging, PCA, and random sampling, respectively, across repeated experiments in the subset size range examined ($N_{\text{tr}} = 10–350$), while the loss coresset method consistently retains only < 5% across all subset sizes, as shown in Figure 4.b. In the pairwise comparison of ATBagging with the alternatives, it outperformed the Random and PCA subsets moderately but consistently, with the proportion of trials in which ATBagging out-performed these two remaining between 50–65% for most subset sizes, as shown in Figure 4.b. Due to the poor performance of the loss coresset method, ATBagging outperformed it in nearly all trials with $n > 10$, and in 75% of trials with $N_{\text{tr}} = 10$.

3.3.2 Downselection Performance: QM9

The QM9 dataset was found to pose a far simpler regression task, with subsets demonstrating far higher accuracies as well as far less across-trial variance compared to ERA5. At size $N_{\text{tr}} = 10$, ATBagging subsets demonstrated a 61% accuracy on average, with the random, PCA, and loss coressets achieving 50%, 51%, and 40% respectively, as shown in Figure 5.b. Again, like with the ERA5 dataset, the methods which explicitly account for heterogeneity are the best performing, while the loss coresset method demonstrates the worst performance, despite performing far better than on ERA5. Even with these higher accuracies and reduced variance, the ATBagging subsets outperformed the alternatives on average for every subset size tested, indeed being the best subset in nearly all trials. In the pairwise comparisons, ATBagging handily outperforms the alternatives on this

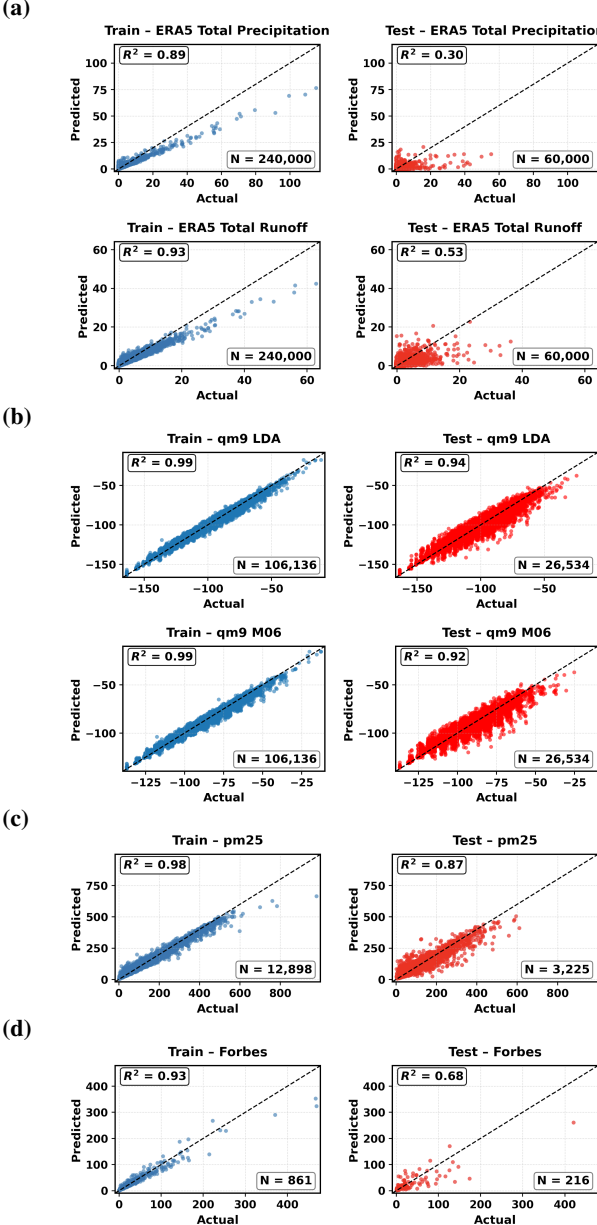


Figure 3: Parity plots demonstrating the capability of the exemplar Scikit-learn RFR model to regress the selected datasets. Each subfigure corresponds to a different dataset utilized in the numerical experiments, with target-transfer datasets appearing twice, once for each target. The left column (blue) represents the training set performance (80% of the data) and the right column (red) represents test set (20% of the data). (a) the ERA5 dataset with source target total precipitation and transfer target total runoff, (b) the QM9 dataset with source target LDA(VWN)-SZP energies and transfer target M06-2X-TZP energies, (c) the PM_{2.5} dataset with target PM_{2.5} particle concentration, and (d) the Forbes 2000 dataset with target market value.

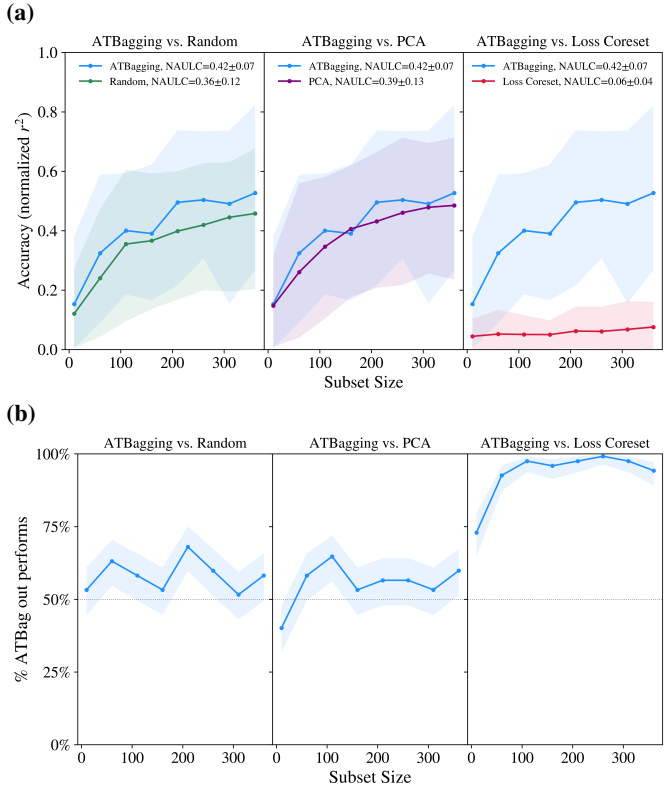


Figure 4: Performance of the subset selection methods for dataset downselection on the ERA5 dataset. (a) Comparison of subset accuracy for those generated by ATBagging to those of the three alternative methods. Mean performance over the replicates is shown as the solid line, with 90% high density intervals shown by the shaded regions. (b) The percentage of trials in which ATBagging outperforms the indicated alternative method. The shaded regions represent 90% credible intervals from a beta-binomial posterior of the pairwise comparison data.

dataset, demonstrating greater accuracy than the alternatives across trials by 65%–98%, as shown in Figure 5.b.

3.3.3 Downselection Performance: Forbes

The Forbes dataset differs from the first two datasets in that it is the first where ATBagging does not outperform or tie across all subset sizes. In this case, ATBagging reaches a plateau in accuracy early, at $N_{tr} = 100$, from which it does not improve, as shown in Figure 6.b. Prior to this plateau, for the small subset sizes, ATBagging outperforms all the alternatives handily, demonstrating 75%–80% outperformance in the pairwise comparisons, as shown in Figure 6.b, due to its +0.1–0.2 difference in accuracy. For subsets larger than these small sizes the alternative methods also plateau similarly, reaching higher accuracies than ATBagging in the case of the PCA and loss coresset methods, while it was lower for the random subset. These results can be understood by considering that this dataset’s features are mixed categorical and numerical, and thus the distance-driven kernel similarity which powers the heterogeneity-enforcing DPP in the ATBagging method is rendered less powerful due to the ambiguous “distance” between categorical features. PCA ignores these small categorical dimensions as not contributing strongly to the variance, and the loss coresset method does not consider these at all. ATBagging

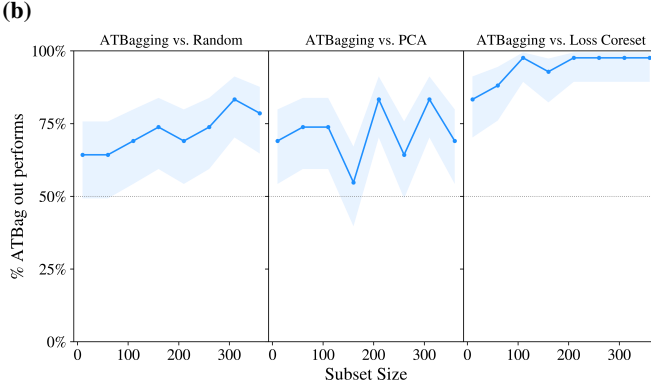
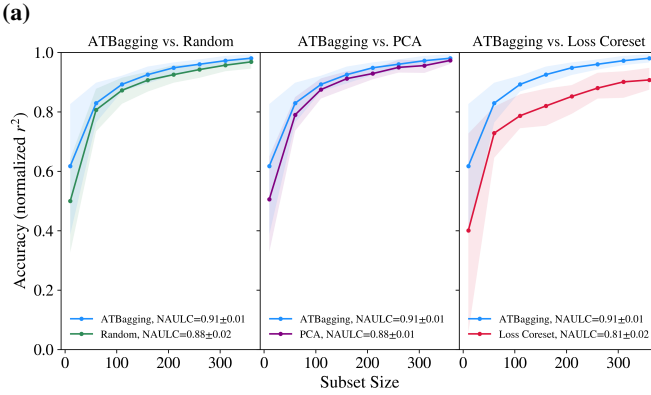


Figure 5: Performance of the subset selection methods for dataset downselection on the QM9 dataset. (a) Comparison of subset accuracy for those generated by ATBagging to those of the three alternative methods. Mean performance over the replicates is shown as the solid line, with 90% high density intervals shown by the shaded regions. (b) The percentage of trials in which ATBagging outperforms the indicated alternative method. The shaded regions represent 90% credible intervals from a beta-binomial posterior of the pairwise comparison data.

is not rendered useless by this limitation: it still shows consistently stronger pairwise performance than random subsets. Moreover, the balance between heterogeneity and informativeness in ATBagging is controlled by a tunable hyperparameter; however, to keep comparisons consistent across datasets, we use the default setting throughout.

3.3.4 Downselection Performance: PM_{2.5}

Finally, the PM_{2.5} dataset generates similar behavior to the ERA5 dataset, in which the heterogeneity-enforcing methods perform well, with ATBagging performing the best overall. Also, like ERA5 the loss coresset method performs poorly, demonstrating accuracies < 10% for subsets up to $N_{tr} = 100$, as shown in Figure 7.b. Like all other datasets, ATBagging performs best at the smallest subset sizes, with an advantage of ~ 0.1 in accuracy above the alternatives at $N_{tr} = 10$, which is realized as a 60–80% rate of outperformance in the pairwise comparisons at that size. ATBagging’s pairwise comparison outperformance against the random and PCA subsets ranges between 50–78% across subset sizes and is near 100% against loss coresset subsets, as shown in Figure 7.b.

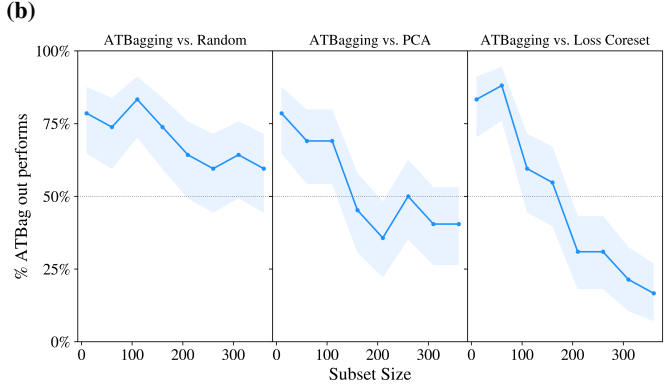
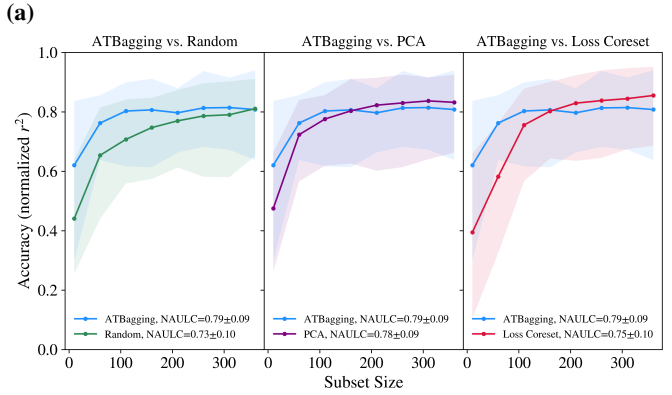


Figure 6: Performance of the subset selection methods for dataset downselection on the Forbes 2000 dataset. (a) Comparison of subset accuracy for those generated by ATBagging to those of the three alternative methods. Mean performance over the replicates is shown as the solid line, with 90% high density intervals shown by the shaded regions. (b) The percentage of trials in which ATBagging outperforms the indicated alternative method. The shaded regions represent 90% credible intervals from a beta-binomial posterior of the pairwise comparison data.

3.3.5 Overall Performance in Data Set Downselection

Our analysis reveals the capability of the ATBagging method to select performant small subsets from real-world datasets of differing types from different domains, while consistently out-performing alternative methods. We find that this outperformance is largely irrespective of the subset size, being violated only in a situation where our specific implementation of kernel similarity does not map nicely to the data (i.e. categorical features). Even in this scenario, ATBagging achieved a higher rate of success compared to alternatives on the smallest subset sizes, indicative of its high utility for low-data scenarios where the cost of data acquisition might preclude the availability of larger subset sizes.

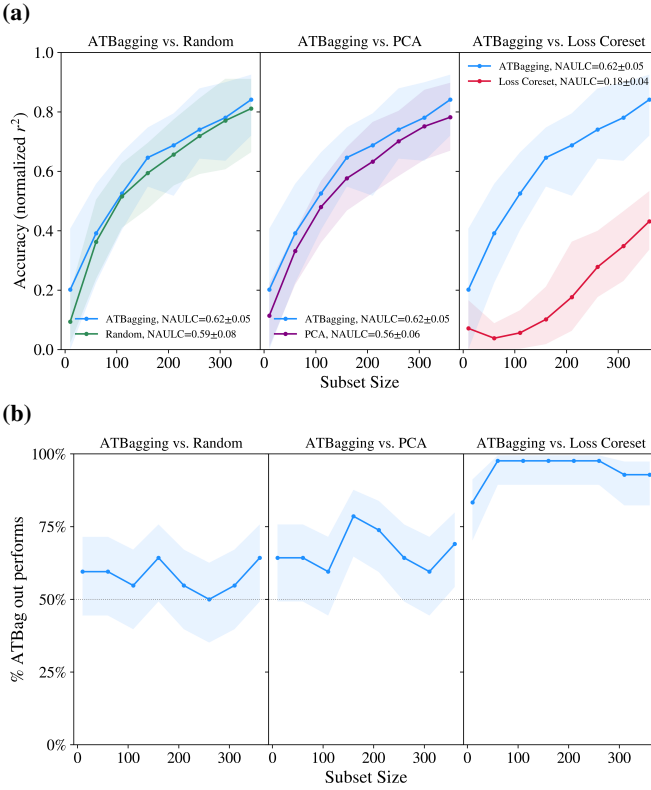


Figure 7: Performance of the subset selection methods for dataset downselection on the PM_{2.5} dataset. (a) Comparison of subset accuracy for those generated by ATBagging to those of the three alternative methods. Mean performance over the replicates is shown as the solid line, with 90% high density intervals shown by the shaded regions. (b) The percentage of trials in which ATBagging outperforms the indicated alternative method. The shaded regions represent 90% credible intervals from a beta-binomial posterior of the pairwise comparison data.

3.4 Transfer & AL Performance

With the quality of the subsets produced by ATBagging demonstrated on the source datasets, we examine performance of the seed subsets for transfer active learning. This is tested for seed subset sizes of $n_{\text{seed}} = 10, 50, 100$ on the four source datasets.

3.4.1 Transfer Seed Subset Performance: QM9

The task for the QM9 dataset was to generate an active learning seed subset of candidate molecules for performing an expensive high accuracy quantum chemical calculation from a dataset containing only a computationally cheap approximation of the more expensive desired target. In this task, the domain dataset remained unchanged (i.e. the set of molecules is the same for both the source and transfer tasks). The initial transfer performance (ITP) on different transfer subsets is shown in Figure 8.c. For all three transferred subset sizes, $n_{\text{seed}} = 10, 50$ and 100, active learning starting from the ATBagging seeds out-perform those from the random, PCA, and loss coresset methods.

Figure 8.c shows the result of active learning from the smallest transfer set, $n_{\text{seed}} = 10$, up to a training set size of 290 via 14 AL acquisition steps each with an acquisition size (m_{collect}) of 20. Such a small n_{seed} was chosen as it demonstrates the most

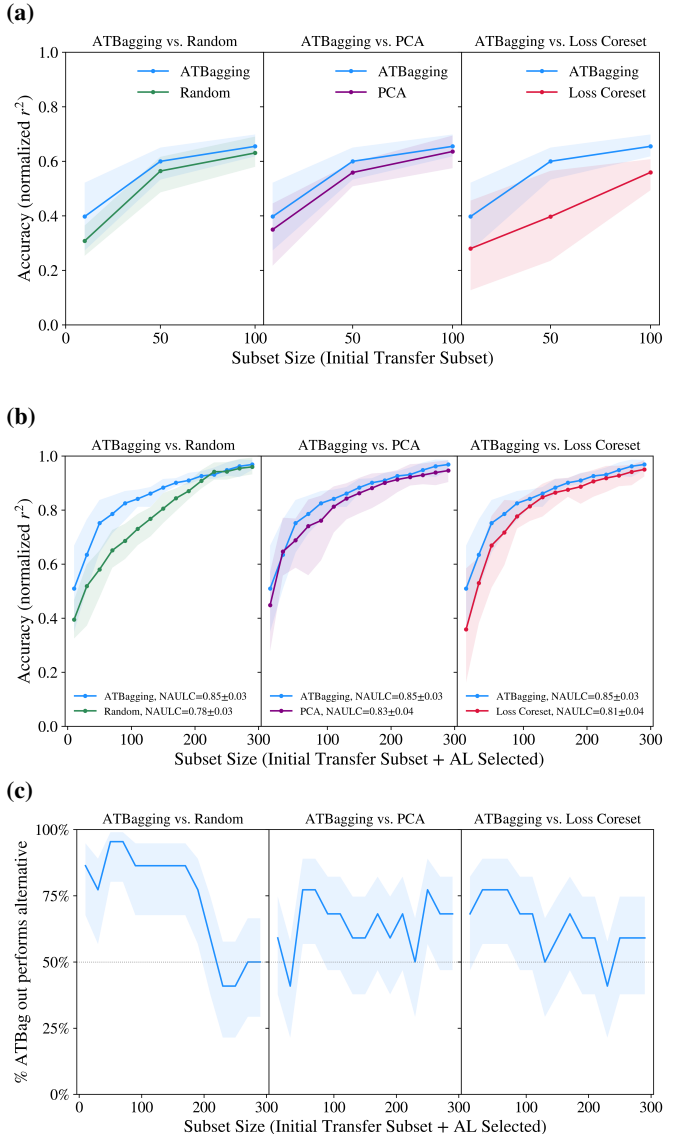


Figure 8: Transfer and active learning performance for the seed subset creation methods on the QM9 dataset. (a) The initial transfer performance (ITP) of RFR models trained on the seed subsets generated by ATBagging and the three alternative methods for seed subset sizes of 10, 50, and 100. (b) Active learning curves starting from n_{seed} of 10 growing with m_{collect} of 20 to a subset of size 290. Mean accuracy is shown as solid lines, with 90% high density intervals shown by the shaded regions. The legend reports the NAULC (mean±std.dev.) of the curves. (c) Pairwise model comparisons, the percentage of trials from the AL trials in (b) in which ATBagging outperformed the indicated alternative method. 90% credible intervals are shown in the shaded regions.

difficult situation for a transfer subset and is where differences between methodologies will be most apparent. The active learning curves for the $n_{\text{seed}} = 50$ and 100 subsets are included in Appendix D. The seed subsets chosen via ATBagging resulted in the highest accuracy of the resulting models, with a NAULC of 0.85 ± 0.03 versus the 0.78 ± 0.03 , 0.83 ± 0.04 , and 0.81 ± 0.04 of subsets generated using the random, PCA, and loss coresset methods, respectively. Thus, ATBagging provides best models with the least data.

The greatest difference in performance is apparent earliest in the active learning process, when the AL acquired training set size (N_{tr}) is below approximately 150 data points, after which the models converge towards similar performance. The quick learning is also seen in the pairwise comparison plot, where ATBagging substantially outperforms random and loss coresset prior to the $N_{\text{tr}} = 150$ mark, as shown in Figure 8.c. PCA demonstrates performance on par with ATBagging at low collected data set sizes, but ATBagging predictions are better after $N_{\text{tr}} = 50$ points collected, and maintains a modest improvement in accuracy and a smaller confidence interval until $N_{\text{tr}} = 300$. This finding demonstrates that the quality of a subset for active learning purposes is not just the accuracy of the model which the subset produces but also the quality of the uncertainty estimates which it produces.

3.4.2 Transfer Seed Subset Performance: PM_{2.5}

The transfer task for the PM_{2.5} dataset is a feature shift task, in which a model trained on a dataset of particulate matter readings from a trial period is used to select a set of locations and times to record particulate matter in the future. This is an example of a feature shift task, where the set of input points are potentially different between the source and transfer. ITP (Figure 9.c) shows a modest advantage towards ATBagging at $n_{\text{seed}} = 10$ and 100 compared to random and PCA subsets, and at all sizes compared to loss coresset subsets. At $n_{\text{seed}} = 50$, both random subset selection and PCA outperform ATBagging in ITP. It is important to note that the ATBagging $n_{\text{seed}} = 50$ subsets outperformed the PCA and random $n_{\text{seed}} = 50$ subsets on the source domain task, indicating that downselection performance does not ensure transfer performance.

ATBagging achieves a modestly higher AL performance than the other methods for the $n_{\text{seed}} = 10$ subsets. It has an NAULC of 0.60 ± 0.08 compared to 0.57 ± 0.05 for PCA and loss coresset subsets, and 0.56 ± 0.07 for random subsets, as shown in Figure 9.c. This is evident in the AL learning curve, which shows the ATBagging subsets averaging slightly above those of the other methods, with loss coresset achieving similar performance earlier in the AL process ($N_{\text{tr}} < 150$). This is also apparent in the pairwise comparisons (Figure 9.c), where ATBagging maintains a roughly 60% lead on average against the random and PCA subsets. A modest lead is also seen in the pairwise comparisons against the loss coresset subsets, but the 50% line remains within the 90% credible intervals for the full learning trajectory.

3.4.3 Transfer Seed Subset Performance: Forbes

The transfer task for the Forbes dataset involves using a model trained on a variety of indicators about Western companies to select which Asian companies to acquire market value to train a performant model for the Asian market. In this task there is no

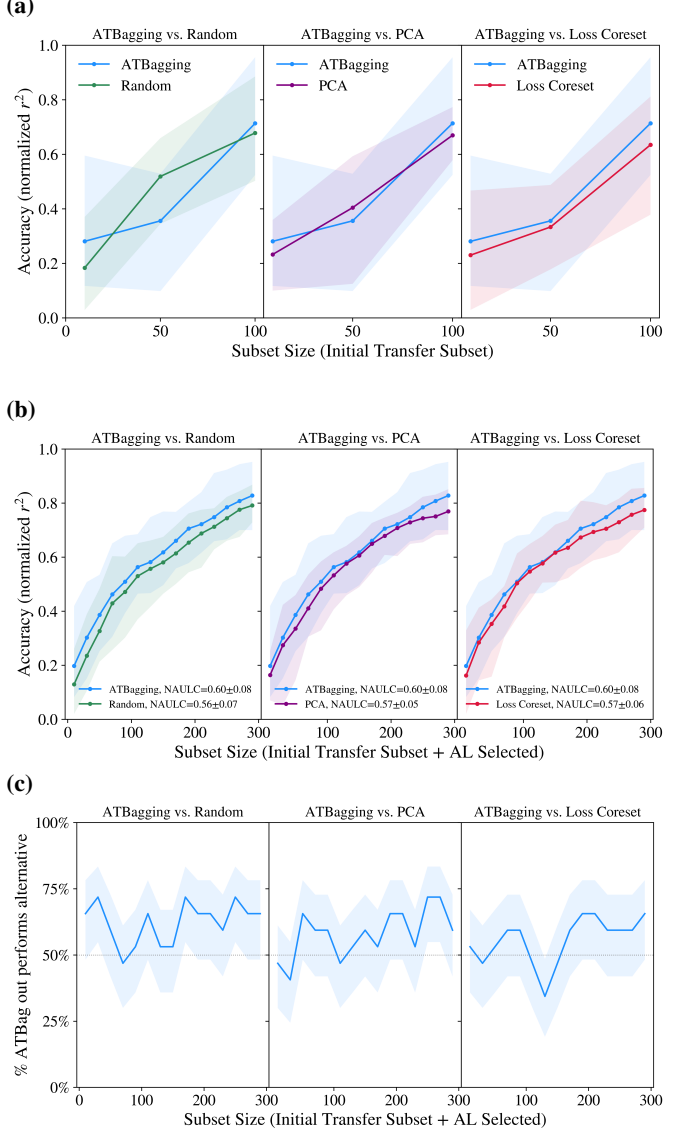


Figure 9: Transfer and active learning performance for the seed subset creation methods on the PM_{2.5} dataset. (a) The initial transfer performance (ITP) of RFR models trained on the seed subsets generated by ATBagging and the three alternative methods for seed subset sizes of 10, 50, and 100. (b) Active learning curves starting from n_{seed} of 10 growing with m_{collect} of 20 to a subset of size 290. Mean accuracy is shown as solid lines, with 90% high density intervals shown by the shaded regions. The legend reports the NAULC (mean \pm std.dev.) of the curves. (c) Pairwise model comparisons, the percentage of trials from the AL trials in (b) in which ATBagging outperformed the indicated alternative method. 90% credible intervals are shown in the shaded regions.

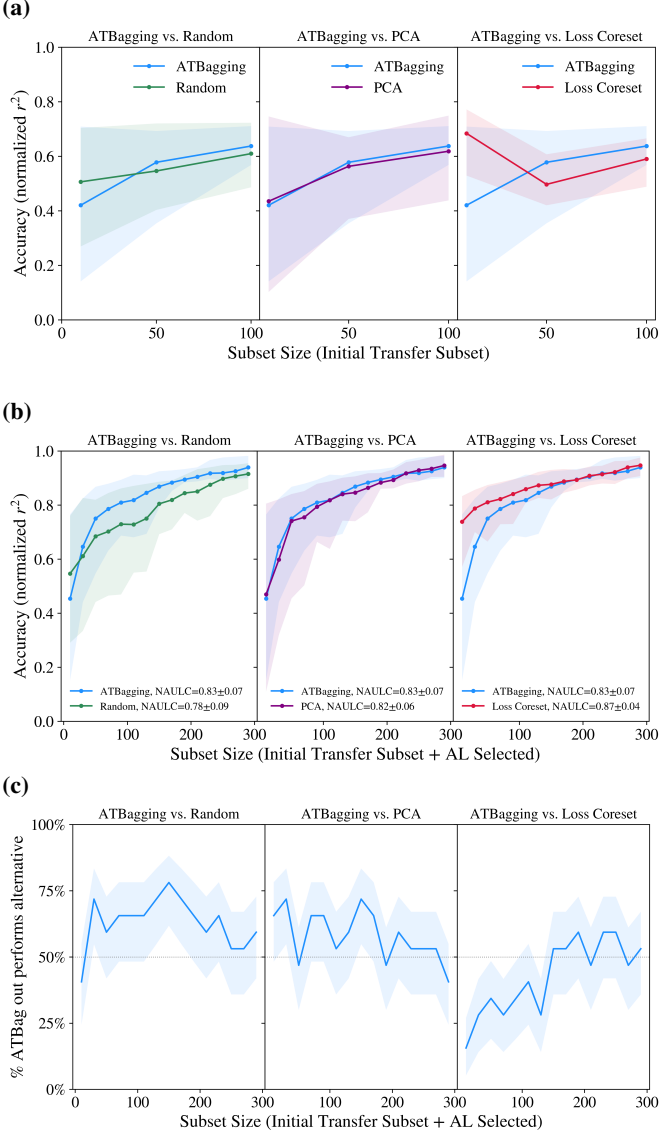


Figure 10: Transfer and active learning performance for the seed subset creation methods on the Forbes 2000 dataset. (a) The initial transfer performance (ITP) of RFR models trained on the seed subsets generated by ATBagging and the three alternative methods for seed subset sizes of 10, 50, and 100. (b) Active learning curves starting from $n_{seed} = 10$ growing with $m_{collect} = 20$ to a subset of size 290. Mean accuracy is shown as solid lines, with 90% high density intervals shown by the shaded regions. The legend reports the NAULC (mean \pm std.dev.) of the curves. (c) Pairwise model comparisons, the percentage of trials from the AL trials in (b) in which ATBagging outperformed the indicated alternative method. 90% credible intervals are shown in the shaded regions.

overlap between the source and transfer datasets (no companies are both Western and Asian). This was the dataset on which ATBagging performed the worst in the downselection task. The ITP is quite similar between ATBagging and PCA subsets, while ATBagging slightly outperforms the random subset generation at the two larger subset sizes, as shown in Figure 10.c. Loss coresset subsets, on the other hand, is significantly different at the smallest subset size, where it outperforms all other methods with a mean accuracy of ~ 0.7 . However, this advantage is quickly lost at the two larger subset sizes (Figure 10.c).

AL performance is dominated by the loss coresset subsets, which exhibit a NAULC of 0.87 ± 0.04 , compared to 0.83 ± 0.07 , 0.82 ± 0.06 , and 0.78 ± 0.09 for the ATBagging, PCA, and random subsets (for $n_{seed} = 10$), respectively (Figure 10.c). Consistent with the ITP, loss coresset and the random subsets both initially outperformed those of ATBagging. However, after the first iteration of active learning ATBagging outperforms the random subset for the rest of the learning curve. On the other hand, the loss coresset subsets maintain their higher performance over ATBagging in this dataset until $N_{tr} = 150$ when both methods converge in accuracy. While the learning curve indicates quite similar performance between ATBagging and PCA subsets, there is a marginal pairwise performance advantage for ATBagging until an N_{tr} of approximately 200 after which their accuracy converges.

3.4.4 Transfer Seed Subset Performance: ERA5

The transfer task for the ERA5 weather dataset is to use a dataset of spatial meteorological data including a target related to precipitation runoff to select locations for measuring a new precipitation-related target. In this task the source and transfer domains are identical. In ITP, ATBagging subsets significantly outperform both PCA and loss coresset subsets at $n_{seed} = 50$ and 100, though it loses to all three competitors when the transferred subset only has $n_{seed} = 10$. At the random subset outperforms ATBagging subsets at all but $n_{seed} = 50$ (Figure 11.c).

AL performance initially mirrors that of ITP, where ATBagging starts with an accuracy of ~ 0.2 , below all other methods. However, in all cases, ATBagging surpasses the competitor methods in accuracy by the time the AL subset reaches $N_{tr} = 100$, after which it maintains superior performance in all three comparisons, as shown in Figure 11.c. NAULC values reflect this trend, with ATBagging subsets scoring the highest at 0.58 ± 0.08 , with random, PCA, and loss coresset subsets following with 0.55 ± 0.12 , 0.55 ± 0.12 , and 0.49 ± 0.08 , respectively (Figure 11.c). The pairwise comparisons (Figure 11.c) demonstrate the superiority of ATBagging for this problem type. The ATBagging subsets outperform those of the loss coreset method 60–85% of the time after $N_{tr} > 100$, as shown in Figure 11.c. ATBagging subsets have a lesser, but still notable, advantage against the random and PCA-generated subsets of approximately 60% after $N_{tr} > 100$.

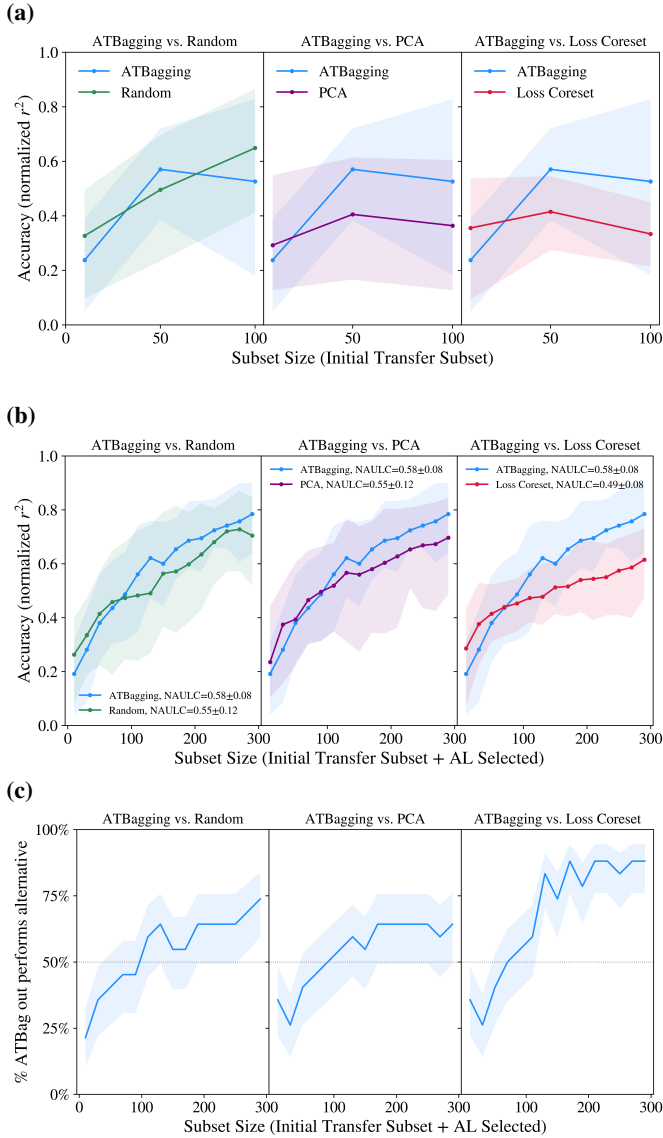


Figure 11: Transfer and active learning performance for the seed subset creation methods on the ERA5 dataset. **(a)** The initial transfer performance (ITP) of RFR models trained on the seed subsets generated by ATBagging and the three alternative methods for seed subset sizes of 10, 50, and 100. **(b)** Active learning curves starting from n_{seed} of 10 growing with m_{collect} of 20 to a subset of size 290. Mean accuracy is shown as solid lines, with 90% high density intervals shown by the shaded regions. The legend reports the NAULC (mean \pm std.dev.) of the curves. **(c)** Pairwise model comparisons, the percentage of trials from the AL trials in **(b)** in which ATBagging outperformed the indicated alternative method. 90% credible intervals are shown in the shaded regions.

3.5 Discussion

Our analysis clearly shows the superior performance of ATBagging subsets for transfer-active learning, especially in target-transfer types of problems (QM9 and ERA5 datasets). Notably, the advantage of our method does not end with its superior downselection performance but extends to advantages in active transfer learning tasks as well, with model accuracy consistently higher even after tens of AL iterations. On feature shift problems, even when initial transfer performance is outclassed by

other methods, the ATBagging subset can match or out-perform the accuracy of other subsets within as few as one AL iteration (e.g. Forbes dataset).

4 CONCLUSIONS

Herein we have developed and demonstrated a novel ATBagging method; by maximizing both the informativeness and heterogeneity of data subsets in downselection and transfer-active learning, ATBagging achieves superior performance in tests on four real-world datasets in both feature-shift and target-transfer type tasks.

Across the tests, the subsets produced by ATBagging were found to be more representative of the source datasets than those of the alternative methods, which acted as more performant seeds in transfer active learning. In downselection of the representative subsets it retained higher accuracy, especially at small N_{tr} , than alternative methods, indicating that the combination of informativeness & feature-space heterogeneity is a strong avenue for dataset distillation.

In transfer-active learning, ATBagging-derived subsets generally demonstrated improved ITP and NAULC, even in cases where it was not the best performing method with low data, it overtook the alternatives within the first 100-150 acquisitions. This suggests that not only does ATBagging generate small n model subsets whose accuracy is generally high, but that it provides excellent starting ground for active learning. Even when the accuracy of predictions based on ATBagging seed data is lower than alternatives, the uncertainty estimates still outperform those of the more accurate same- n models in determining which points to select next.

Overall, these results show that ATBagging is a practical methodology for the transfer-active learning task, especially in scenarios where the cost of dataset labelling is expensive, forcing the problem into the low n regime where it performs most favorably.

Table 2: Comparison of Method Performances on Transfer Learning Seed Creation

Dataset	Subset Size (n_{seed})	Metric	Random	PCA	Loss Coreset	ATBagging
QM9	10	ITP	0.31	0.35	0.28	0.40
		NAULC	0.61	0.65	0.63	0.66
	50	ITP	0.56	0.56	0.40	0.60
		NAULC	0.70	0.68	0.65	0.71
	100	ITP	0.63	0.64	0.56	0.66
		NAULC	0.67	0.67	0.60	0.68
	PM _{2.5}	ITP	0.18	0.23	0.23	0.28
		NAULC	0.68	0.68	0.61	0.72
Forbes	10	ITP	0.52	0.40	0.33	0.36
		NAULC	0.72	0.64	0.69	0.71
	50	ITP	0.68	0.67	0.63	0.71
		NAULC	0.80	0.60	0.56	0.66
	100	ITP	0.51	0.44	0.68	0.42
		NAULC	0.72	0.76	0.81	0.77
	50	ITP	0.55	0.56	0.50	0.58
		NAULC	0.61	0.61	0.59	0.63
ERA5	100	ITP	0.61	0.62	0.59	0.64
		NAULC	0.62	0.64	0.64	0.64
	10	ITP	0.33	0.29	0.36	0.24
		NAULC	0.68	0.68	0.61	0.72
	50	ITP	0.50	0.41	0.42	0.57
		NAULC	0.72	0.64	0.69	0.71
	100	ITP	0.65	0.36	0.33	0.53
		NAULC	0.80	0.60	0.56	0.66
			Wins	6	0	15

FUNDING SOURCES

The Authors gratefully acknowledge several funding sources which supported the authors contributing to this cross-project collaborative effort. VP acknowledges support from the Science and Technologies for Phosphorus Sustainability (STEPS) Center, a National Science Foundation Science and Technology Center (CBET-2019435). DR acknowledges support from the National Alliance for Water Innovation (NAWI), funded by the U.S. Department of Energy, Office of Energy Efficiency and Renewable Energy (EERE), Industrial Technologies Office (ITO), under Funding Opportunity Announcement DE-FOA-0001905 and from the U.S. National Science Foundation CBET Catalysis under award 2450869. ON acknowledges support from the National Institute of Environmental Health Sciences of the National Institutes of Health under Award Number P42ES030990 as part of the MEMCARE (Metals Mixtures: Cognitive Aging, Remediation, and Exposure Sources) project and the National Science Foundation Nanosystems Engineering Research Center for Nanotechnology Enabled Water Treatment (NEWT EEC 1449500). SW acknowledge support from the U.S. Department of Energy's Energy Efficiency & Renewable Energy office under Award Number DE-EEDE-EE0010732 and the U.S. Department of Energy, Office of Science under Federal Award Identification Number DE-SC0024724. CM acknowledge support from the U.S. Department of Energy, Office of Science, Office of Basic Energy Sciences, under Award Number(s) DE-SC0024194. The content is solely the authors' responsibility and does not necessarily represent the official views of the National Institutes of Health, US Department of Energy, or the NSF. In addition, we acknowledge support from Research Comput-

ing at Arizona State University for providing high-performance supercomputing services.[40]

CODE AVAILABILITY

A python package which implements a Scikit-learn compatible implementation of the ATBagging methodology is available on github at:
https://github.com/MuhichLab/active_transfer_bagging

CORRESPONDING AUTHOR INFORMATION

Corresponding Authors: Christopher Muhich
 Email: cmuhich@asu.edu
 Telephone: 480-965-2673
 Address: 551 E. Tyler Mall, ERC 257, Arizona State University, Tempe AZ

REFERENCES

[1] Yuji Roh, Geon Heo, and Steven Euijong Whang. A survey on data collection for machine learning: A big data - ai integration perspective. *IEEE Transactions on Knowledge and Data Engineering*, 33:1328–1347, 4 2021. ISSN 1041-4347. doi:10.1109/TKDE.2019.2946162.

[2] Zeyad Emam, Andrew Kondrich, Sasha Harrison, Felix Lau, Yushi Wang, Aerin Kim, and Elliot Branson. On the state of data in computer vision: Human annotations remain indispensable for developing deep learning models. 7 2021.

[3] Tim Rädsch, Annika Reinke, Vivienn Weru, Minu D. Tizabi, Nicholas Schreck, A. Emre Kavur, Bünyamin Pekdemir, Tobias Roß, Annette Kopp-Schneider, and Lena Maier-Hein. Labelling instructions matter in biomedical image analysis. *Nature Machine Intelligence*, 5:273–283, 3 2023. ISSN 2522-5839. doi:10.1038/s42256-023-00625-5.

[4] Alistair Lawley, Rory Hampson, Kevin Worrall, and Gordon Dobie. A cost focused framework for optimizing collection and annotation of ultrasound datasets. *Biomedical Signal Processing and Control*, 92:106048, 6 2024. ISSN 17468094. doi:10.1016/j.bspc.2024.106048.

[5] John A. Keith, Valentin Vassilev-Galindo, Bingqing Cheng, Stefan Chmiela, Michael Gastegger, Klaus-Robert Müller, and Alexandre Tkatchenko. Combining machine learning and computational chemistry for predictive insights into chemical systems. *Chemical Reviews*, 121:9816–9872, 8 2021. ISSN 0009-2665. doi:10.1021/acs.chemrev.1c00107.

[6] Shikun Zhang, Omid Jafari, and Parth Nagarkar. A survey on machine learning techniques for auto labeling of video, audio, and text data. 9 2021.

[7] Alaa Tharwat and Wolfram Schenck. A survey on active learning: State-of-the-art, practical challenges and research directions. *Mathematics*, 11:820, 2 2023. ISSN 2227-7390. doi:10.3390/math11040820.

[8] Dmitriy Dligach and Martha Palmer. Good seed makes a good crop: accelerating active learning using language modeling. In *Proceedings of the 49th Annual Meeting of the Association for Computational Linguistics: Human Language Technologies: Short Papers - Volume 2*, pages 6–10. Association for Computational Linguistics, 2011. ISBN 9781932432886.

[9] Akshay L Chandra, Sai Vikas Desai, Chaitanya Devaguptapu, and Vineeth N Balasubramanian. On initial pools for deep active learning. 7 2021.

[10] Rong Hu, Brian Mac Namee, and Sarah Jane Delany. Off to a good start: Using clustering to select the initial training set in active learning. In *Proceedings of the 23rd International Florida Artificial Intelligence Research Society Conference, FLAIRS-23*, pages 26–31, 2010. ISBN 9781577354475. doi:10.21427/d7q89w.

[11] V. Diana Rakotonirina, Marco Bragato, Guido Falk von Rudorff, and O. Anatole von Lilienfeld. Hammett-inspired product baseline for data-efficient δ -ml in chemical space. 5 2025.

[12] Clemens-Alexander Brust, Christoph Käding, and Joachim Denzler. Active and incremental learning with weak supervision. *KI - Künstliche Intelligenz*, 34:165–180, 6 2020. ISSN 0933-1875. doi:10.1007/s13218-020-00631-4.

[13] Dong, Roth Holger R., Xu Daguang Nath Vishwesh, and Yang. Warm start active learning with proxy labels and selection via semi-supervised fine-tuning. In Qi, Fletcher P Thomas, Speidel Stefanie, Li Shuo Wang Linwei, and Dou, editors, *Medical Image Computing and Computer Assisted Intervention – MICCAI 2022*, pages 297–308. Springer Nature Switzerland, 2022. ISBN 978-3-031-16452-1.

[14] Olivier Bachem, Mario Lucic, and Andreas Krause. Coresets for nonparametric estimation: the case of dp-means. In *Proceedings of the 32nd International Conference on International Conference on Machine Learning - Volume 37*, pages 209–217. JMLR.org, 2015.

[15] Pang Wei Koh and Percy Liang. Understanding black-box predictions via influence functions. 12 2020.

[16] Vladimir Braverman, Dan Feldman, Harry Lang, Adiel Statman, and Samson Zhou. Efficient coresets constructions via sensitivity sampling. In Vineeth N Balasubramanian and Ivor Tsang, editors, *Proceedings of The 13th Asian Conference on Machine Learning*, volume 157, pages 948–963. PMLR, 11 2021. URL <https://proceedings.mlr.press/v157/braverman21a.html>.

[17] Andreas Kirsch, Joost van Amersfoort, and Yarin Gal. Batchbald: Efficient and diverse batch acquisition for deep bayesian active learning. 10 2019.

[18] David Holzmüller, Viktor Zaverkin, Johannes Kästner, and Ingo Steinwart. A framework and benchmark for deep batch active learning for regression. *Journal of Machine Learning Research*, 24:1–81, 2023. URL <http://jmlr.org/papers/v24/22-0937.html>.

[19] S. Kullback and R. A. Leibler. On information and sufficiency. *The Annals of Mathematical Statistics*, 22:79–86, 3 1951. ISSN 0003-4851. doi:10.1214/aoms/1177729694.

[20] Freddie Bickford Smith, Andreas Kirsch, Sebastian Farquhar, Yarin Gal, Adam Foster, and Tom Rainforth. Prediction-oriented bayesian active learning. *International Conference on Artificial Intelligence and Statistics*, 2023.

[21] Leo Breiman. Bagging predictors. *Machine Learning*, 24:123–140, 8 1996. ISSN 0885-6125. doi:10.1007/BF00058655.

[22] Alex Kulesza. Determinantal point processes for machine learning. *Foundations and Trends® in Machine Learning*, 5:123–286, 2012. ISSN 1935-8237. doi:10.1561/2200000044.

[23] Ali Rahimi and Benjamin Recht. Random features for large-scale kernel machines. In *Proceedings of the 21st International Conference on Neural Information Processing Systems*, pages 1177–1184. Curran Associates Inc., 2007. ISBN 9781605603520.

[24] J Muñoz-Sabater, E Dutra, A Agust{1}-Panareda, C Albergel, G Arduini, G Balsamo, S Boussetta, M Choulga, S Harrigan, H Hersbach, B Martens, D G Miralles, M Piles, N J Rodr{1}guez-Fernández, E Zsoter, C Buontempo, and J.-N. Thépaut. Era5-land: a state-of-the-art

global reanalysis dataset for land applications. *Earth System Science Data*, 13:4349–4383, 2021. doi:10.5194/essd-13-4349-2021. URL <https://essd.copernicus.org/articles/13/4349/2021/>.

[25] Surajit Nandi, Tejs Vegge, and Arghya Bhowmik. Multix-cqm9: Large dataset of molecular and reaction energies from multi-level quantum chemical methods. *Scientific Data*, 10:783, 11 2023. ISSN 2052-4463. doi:10.1038/s41597-023-02690-2.

[26] Forbes. The global 2000, 2025. URL <https://www.forbes.com/lists/global2000/>.

[27] Xuan Liang, Tao Zou, Bin Guo, Shuo Li, Haozhe Zhang, Shuyi Zhang, Hui Huang, and Song Xi Chen. Assessing beijing's pm $_{2.5}$ pollution: severity, weather impact, apec and winter heating. *Proceedings of the Royal Society A: Mathematical, Physical and Engineering Sciences*, 471:20150257, 10 2015. ISSN 1364-5021. doi:10.1098/rspa.2015.0257.

[28] P.C. Mahalanobis. Reprint of: Mahalanobis, p.c. (1936) "on the generalised distance in statistics.". *Sankhya A*, 80: 1–7, 12 2018. ISSN 0976-836X. doi:10.1007/s13171-019-00164-5.

[29] Zhexue Huang. Extensions to the k-means algorithm for clustering large data sets with categorical values. *Data Mining and Knowledge Discovery*, 2:283–304, 9 1998. ISSN 1384-5810. doi:10.1023/A:1009769707641.

[30] Baharan Mirzasoleiman, Jeff Bilmes, and Jure Leskovec. Coresets for data-efficient training of machine learning models. In *Proceedings of the 37th International Conference on Machine Learning*. JMLR.org, 2020.

[31] Ming-Hui Chen, Joseph G. Ibrahim, and Sungduk Kim. Properties and implementation of jeffreys's prior in binomial regression models. *Journal of the American Statistical Association*, 103:1659–1664, 12 2008. ISSN 0162-1459. doi:10.1198/016214508000000779.

[32] Trevor. Hastie, J. H. Friedman, and Robert. Tibshirani. *The elements of statistical learning : data mining, inference, and prediction*. Springer, 2009. ISBN 0387952845.

[33] Jem J., King Ross D Burbidge Robert, and Rowland. Active learning for regression based on query by committee. In Peter, Corchado Emilio, Byrne Will, Yao Xin Yin Hujun, and Tino, editors, *Intelligent Data Engineering and Automated Learning - IDEAL 2007*, pages 209–218. Springer Berlin Heidelberg, 2007. ISBN 978-3-540-77226-2.

[34] Andreas Kirsch. Black-box batch active learning for regression. *Transactions on Machine Learning Research*, 7 2022.

[35] F Pedregosa, G Varoquaux, A Gramfort, B Michel V., Thirion, O Grisel, M Blondel, R Prettenhofer P., Weiss, V Dubourg, J Vanderplas, A Passos, D Cournapeau, M Brucher, M Perrot, and E Duchesnay. Scikit-learn: Machine learning in python. *Journal of Machine Learning Research*, 12:2825–2830, 2011.

[36] Alex Kulesza and Ben Taskar. k-dpps: fixed-size determinantal point processes. In *Proceedings of the 28th International Conference on International Conference on Machine Learning*, pages 1193–1200. Omnipress, 2011. ISBN 9781450306195.

[37] Simon Barthélémy, Pierre-Olivier Amblard, and Nicolas Tremblay. Asymptotic equivalence of fixed-size and varying-size determinantal point processes. *Bernoulli*, 25, 11 2019. ISSN 1350-7265. doi:10.3150/18-BEJ1102.

[38] Nicolas Tremblay, Simon Barthélémy, and Pierre-Olivier Amblard. Optimized algorithms to sample determinantal point processes. 2 2018.

[39] R. P.. Brent. *Algorithms for minimization without derivatives*. Prentice-Hall, 1973. ISBN 0130223352.

[40] Douglas M. Jennewein, Johnathan Lee, Chris Kurtz, Will Dizon, Ian Shaefner, Alan Chapman, Alejandro Chiquete, Josh Burks, Amber Carlson, Natalie Mason, Arhat Kobwala, Thirugnanam Jagadeesan, Praful Barghav, Torey Battelle, Rebecca Belshe, Debra McCaffrey, Marisa Brazil, Chaitanya Inumella, Kirby Kuznia, Jade Buzinski, Sean Dudley, Dhruvil Shah, Gil Speyer, and Jason Yalim. The Sol Supercomputer at Arizona State University. In *Practice and Experience in Advanced Research Computing*, PEARC '23, pages 296–301, New York, NY, USA, Jul 2023. Association for Computing Machinery. ISBN 9781450399852. doi:10.1145/3569951.3597573.

A IN-BAG/OUT-OF-BAG MODEL AVAILABILITY

Following from the definition of a bagged ensemble model as a model $\mathcal{M} = \{m_i\}_i^M$, comprised of M submodels of weak learners, m_i , trained on bootstrapped samples of the training dataset, the probability of a data point's exclusion from a bootstrapped resampling is $\frac{1}{e}$; therefore, the probability of both in-bag and out-of-bag models existing for every point in the dataset of size N is $\left(1 - \left(1 - \frac{1}{e}\right)^M\right)^N$. Thus, even assuming a massive one-million-point data set, the generation of 50 models means that there is only a 1 in 10,000 chance of even a single data point not being present in at least one in- and one out-of-bag model. If 100 models are constructed, a data set of 10 quadrillion points would be necessary to have the same, still tiny, 1 in 10,000 chance of not having both in- and out-of-bag models.

B INFORMATION GAIN VIA BAYESIAN INTERPRETATION OF BAGGING MODELS

Assuming a Bayesian context, where model parameters are treated as random variables with distribution $p(\theta)$, the predictive distributions are expressed via the integral

$$p(Y_*|X_*) = \int p(Y_*|X_*, \theta)p(\theta)d\theta$$

In regression, it is reasonable to partition uncertainty such that all epistemic uncertainty is placed on the parameters, i.e. that the distribution over parameters represents the uncertainty in their true values, and all aleatoric uncertainty is placed on the model predictions, i.e. that the data generation process is noisy. This partitioning is achieved by imposing a Gaussian noise model over model predictions via $p(Y_*|X_*, \theta) \sim \text{MVN}(m_\theta(X_*), \sigma^2 I_n)$, where the mean vector is the vector of model predictions over the input set X_* and σ^2 is the observational noise, a hyperparameter. The integral then becomes,

$$p(Y_*|X_*) = \int \text{MVN}(m_\theta(X_*), \sigma^2)p(\theta)d\theta$$

With a bagged ensemble, the model parameters for in-bag models, θ_{ib} , are approximately drawn from the posterior parameter distribution, $\theta_{\text{ib}} \sim p(\theta|x, y)$, while model parameters for out-of-bag models θ_{oob} are approximately drawn from the prior distribution, $\theta_{\text{oob}} \sim p(\theta)$. Thus, the above integrals may be approximated via a Monte Carlo expectation

$$\begin{aligned} p(Y_*|X_*) &\approx \frac{1}{|\mathcal{M}_{\text{oob}}|} \sum_{m \in \mathcal{M}_{\text{oob}}} \text{MVN}(m(X_*), \sigma^2 I_n) \\ p(Y_*|X_*, x, y) &\approx \frac{1}{|\mathcal{M}_{\text{ib}}|} \sum_{m \in \mathcal{M}_{\text{ib}}} \text{MVN}(m(X_*), \sigma^2 I_n) \end{aligned}$$

These approximations are both mixtures of multivariate Gaussians, which makes calculating their KL divergence intractable. Therefore, the mixture distributions are approximated via a single multivariate Gaussian with matched moments,

$$\begin{aligned} p(Y_*|X_*) &\approx \frac{1}{|\mathcal{M}_{\text{ib/oob}}|} \sum_{m \in \mathcal{M}_{\text{ib/oob}}} \text{MVN}(m(X_*), \sigma^2 I) \approx \text{MVN}(\mu, \Sigma) \\ \mu &= \frac{1}{|\mathcal{M}_{\text{ib/oob}}|} \sum_{m \in \mathcal{M}_{\text{ib/oob}}} m(X_*) \\ \Sigma &= \sigma^2 I_n + \frac{1}{|\mathcal{M}_{\text{ib/oob}}|} \sum_{m \in \mathcal{M}_{\text{ib/oob}}} (m(X_*) - \mu)(m(X_*) - \mu)^\top \end{aligned}$$

With this approximation, the KL divergence and thus information gain upon including data point (x, y) is expressible analytically as:

$$\text{KL}(p(Y_*|X_*, x, y) \parallel p(Y_*|X_*)) = \frac{1}{2}[\text{tr}(\Sigma_{\text{oob}}^{-1}\Sigma_{\text{ib}}) + (\mu_{\text{oob}} - \mu_{\text{ib}})^\top \Sigma_{\text{oob}}^{-1}(\mu_{\text{oob}} - \mu_{\text{ib}}) - n - \ln \frac{\det \Sigma_{\text{oob}}}{\det \Sigma_{\text{ib}}}]$$

This KL divergence is calculated for every point in the training set, the magnitude of which defines its informativeness.

C APPROXIMATE SAMPLING OF ILL-CONDITIONED k -DPPs

In applications where our approach is attractive it is assumed that acquiring labels for the seed subset is either expensive or will take a large amount of time, and therefore budgeting subset acquisition in terms of a predetermined subset size is desirable. This poses a problem with utilizing DPPs for the subset creation, as a sample from a DPP is a subset of random size. This problem of fixed sample size is addressed via k -DPPs, a method of sampling from a DPP conditional on a fixed sample size k . [36] However, as the size of the dataset increases problems may arise with the use k -DPPs, since for rank-deficient L -matrices sampling from a k -DPP may fail for even small k , while the sampling process itself, which depends on an eigendecomposition of the L -matrix, may become computationally prohibitive.

The latter of these problems has been addressed by fast DPP sampling algorithms which exploit the RFF decomposition of the kernel from which the L matrix is constructed, which can be applied for both k -DPP and normal DPP sampling.[37] The first of these issues, the rank deficiency of L which is observed in many real applications such as those utilized as test cases in this work, remains an issue.

To address these issues, we propose the following extension to Algorithm 3 of Tremblay et al. [38] and Algorithm 1 of Kulesza [22], where we scale the L matrix such that the expectation of the sample size of the L -ensemble is equal to our desired sample size. This is done by solving for the scale factor, a , in the equation,

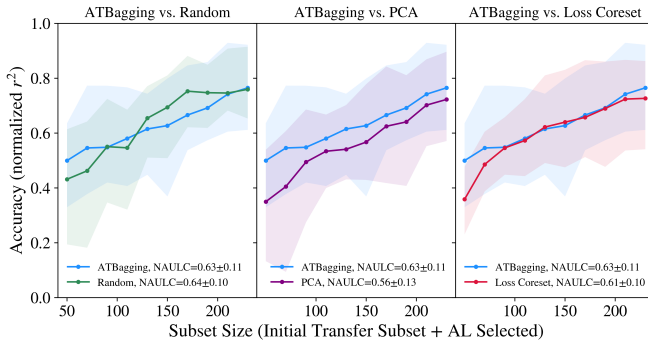
$$\mathbb{E}[|\mathcal{S}|] = \sum_i \frac{a\lambda_i}{1 + a\lambda_i}$$

with the expected sample size $\mathbb{E}[|\mathcal{S}|]$ set to the desired sample size, where λ_i are the eigenvalues of the L matrix. This must be done numerically, which we do via Brent's root finding method.[39] With the scaled eigenvectors of L , they are sampled according to Algorithm 3 and used to construct a projective L -ensemble which may be sampled using a standard technique.

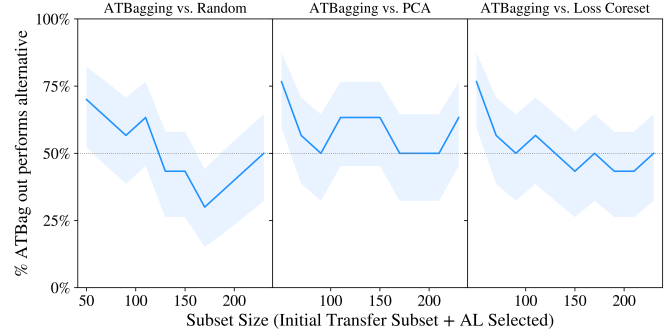
This approach is robust to ill-conditioned L matrices but does come with some drawbacks. As the subset size is still random, there is no guarantee that the first attempt will generate a sample of the desired size, and therefore multiple samples are sometimes required. Additionally, uniform scaling of the L matrix may modify the marginal inclusion probabilities of each point in complicated ways. In practice this was not seen to be an issue, but an improved k -DPP sampling method which can handle ill-conditioned L matrices is desired for future research.

D SUPPLEMENTAL TRANSFER LEARNING FIGURES

Transfer Performance – ERA5: Subset Size 50

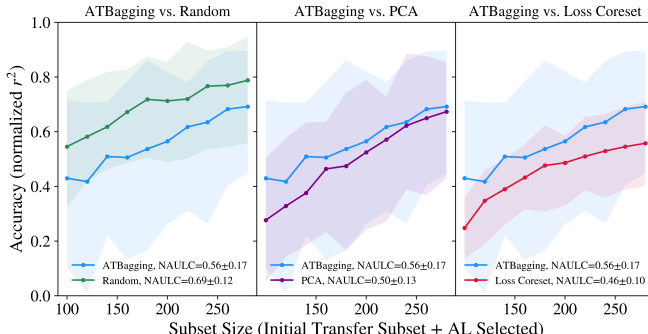


(a) ERA5 dataset transfer performance with initial subset size of 50.

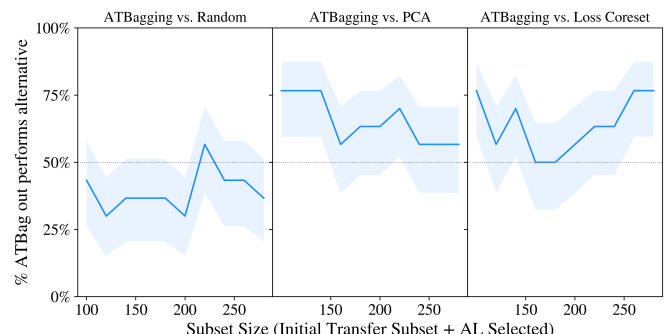


(b) ERA5 dataset transfer performance pairwise method comparisons with initial subset size of 50.

Transfer Performance – ERA5: Subset Size 100

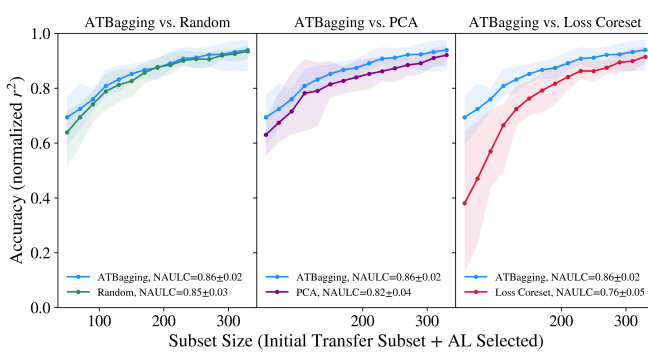


(a) ERA5 dataset transfer performance with initial subset size of 100.

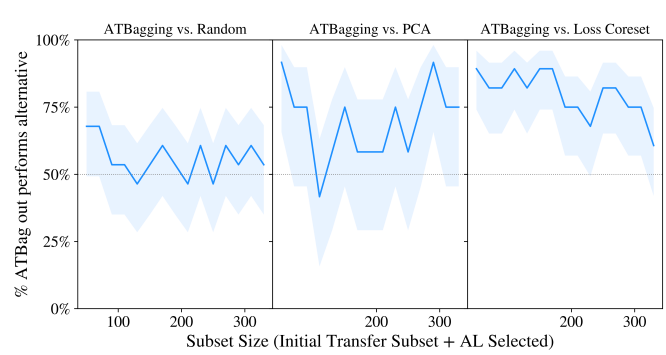


(b) ERA5 dataset transfer performance pairwise method comparisons with initial subset size of 100.

Transfer Performance – QM9: Subset Size 50

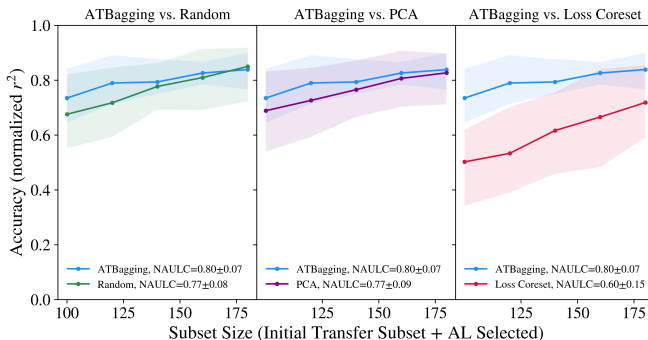


(a) QM9 dataset transfer performance with initial subset size of 50.

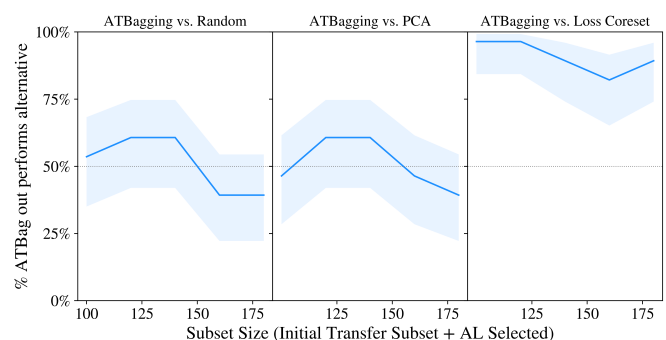


(b) QM9 dataset transfer performance pairwise method comparisons with initial subset size of 50.

Transfer Performance – QM9: Subset Size 100

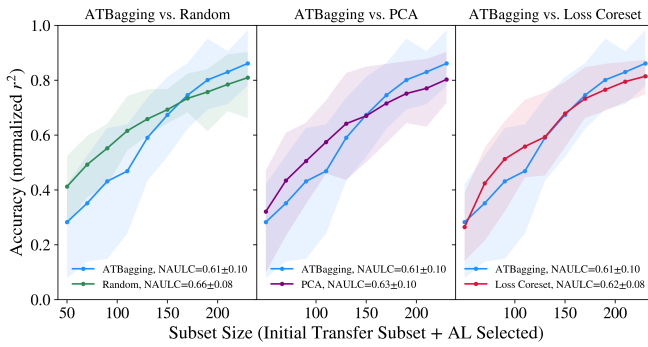


(a) QM9 dataset transfer performance with initial subset size of 100.

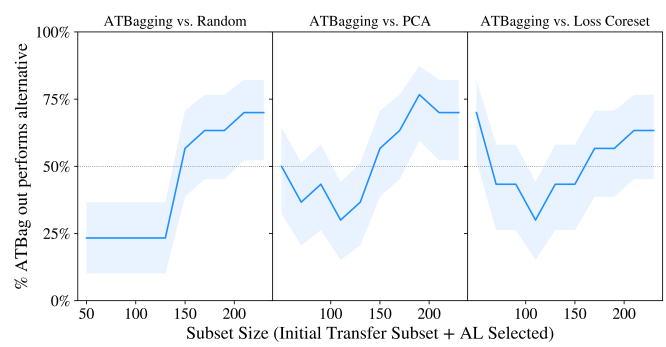


(b) QM9 dataset transfer performance pairwise method comparisons with initial subset size of 100.

Transfer Performance – PM_{2.5}: Subset Size 50

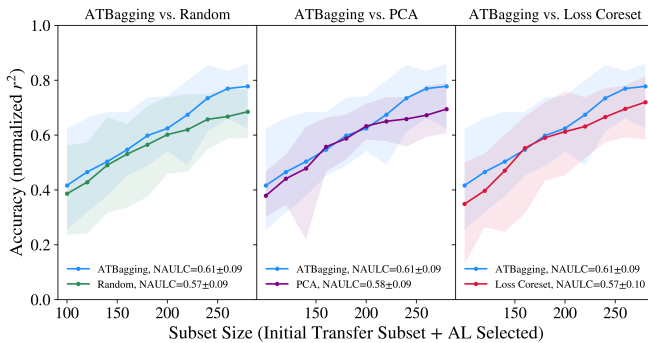


(a) PM_{2.5} dataset transfer performance with initial subset size of 50.

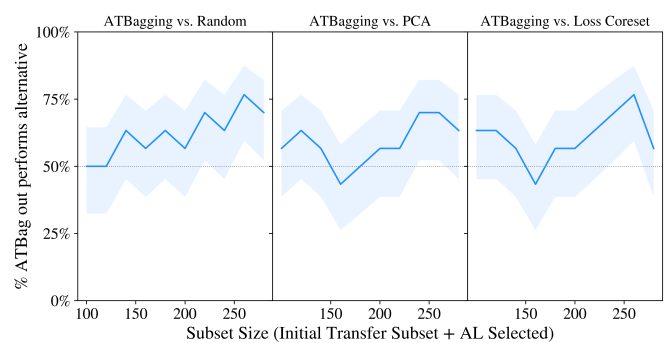


(b) PM_{2.5} dataset transfer performance pairwise method comparisons with initial subset size of 50.

Transfer Performance – PM_{2.5}: Subset Size 100

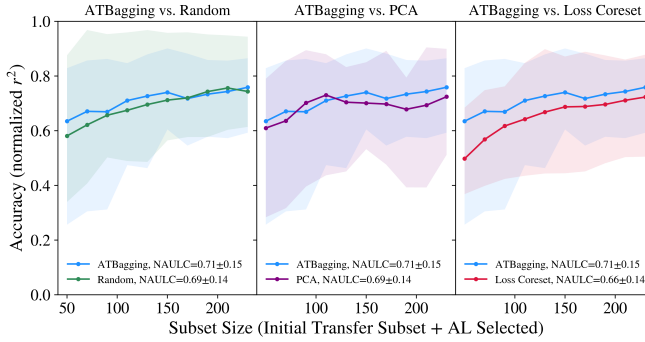


(a) PM_{2.5} dataset transfer performance with initial subset size of 100.

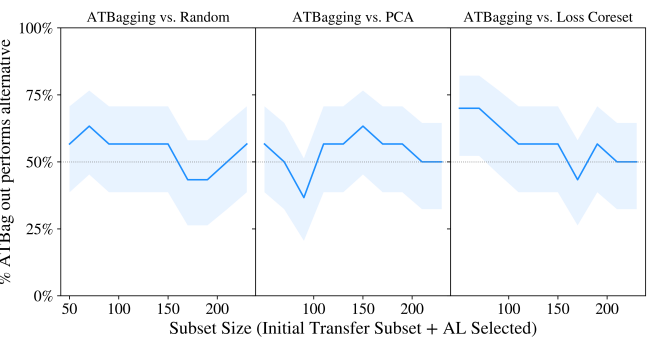


(b) PM_{2.5} dataset transfer performance pairwise method comparisons with initial subset size of 100.

Transfer Performance – Forbes: Subset Size 50

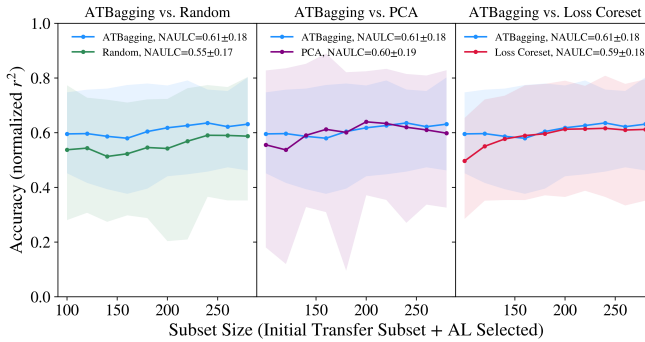


(a) Forbes 2000 dataset transfer performance with initial subset size of 50.

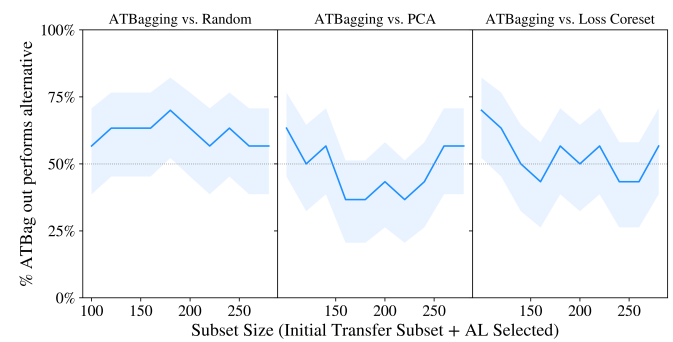


(b) Forbes 2000 dataset transfer performance pairwise method comparisons with initial subset size of 50.

Transfer Performance – Forbes: Subset Size 100



(a) Forbes 2000 dataset transfer performance with initial subset size of 100.



(b) Forbes 2000 dataset transfer performance pairwise method comparisons with initial subset size of 100.